Metal complexes in cancer therapy: Synthesis, spectroscopic characterization and antitumor effect against breast cancer of new dihydroxy phenyl ethylidene amino benzoic acid complexes

Abdou Saad El-Tabl[1], Moshira Mohamed Abd El-Wahed[2] , Emad Mohamed El-Henawy[3] , Omnya Ebrahim Abd El-Wahab[1] and Shaimaa Mohamed Fahim Hashim[1]

[1] Chemistry Department, Faculty of Science, Menoufia University, Egypt.

[2] Pathology Department, Faculty of Medicine, Menoufia University, Egypt.

[3] Pharmacology Department, Faculty of Medicine, Menoufia University, Egypt.

Abstract: Cr(III) , Mn(II), Co(II), Ni(II), Cu(II), Zn(II) and Cd(II) and Ca(II), Fe(III), Hg(II), Pb(II), and Bi(III) complexes of (E)-2- ((1-(5-acetyl-2,4-dihydroxy phenyl) ethylidene) amino) benzoic acid were prepared and characterized by elemental analyses, IR, UV-Vis spectra, Magnetic moments, Conductivity, ^{1}H-NMR and Mass spectra, Thermal analyses (DTA and TGA) and ESR measurements. The analytical and IR data showed that, the ligand behaves as neutral or monobasic tridentate. Molar conductivity in DMF indicate that, the complexes are non-electrolytes. ESR spectra of solid Cu(II) complexes at room temperature show axial type (dx^2-y^2) with covalent bond character in an octahedral environment. However, Co(II), Fe(II) and Mn(II) complexes showed isotropic type. Complexes showed inhibitory activity against breast cancer (MCF-7 cell line) compared with standard drug. Zn(II) complex (8) demonstrated high potency inhibition activity against MCF-7 cell line with IC_{50} (50.2).

Keywords: Complexes; spectral, magnetism, ESR, breast cancer.

INTRODUCTION

Schiff bases have a vital position in metal coordination chemistry even almost a century since their discovery. Due to their simplicity in preparation, diverse properties, medicinal, biochemical and industrial applications, the keen interest in the study of these compounds arose in the recent years. Study of inorganic complexes containing biologically important ligands is made easier, because certain metal ions are active in many biological processes; species of low molecular weight are hence, sought that reproduce as far as possible, the structural properties and the reactivity of naturally occurring complexes of these ions in such processes. It is known that, the existence of metal ions bonded to biologically active compounds may enhance their activities[1]. A number of metal coordination complexes of Schiff bases have been suggested as antibacterial, antifungal, cytotoxic, anti-inflammatory and cytostatic agents[2-5]. In order to widen the scope of investigations on the coordination behavior of various donor ligands including Schiff base towards organo-metallics, we carried out the spectroscopic investigations and established their bioactivities[2, 3, 6-9]. As an extension of this research, here in, we report the synthesis, characterization and antitumor activity against MCF-7 cell line of a Schiff base and its metal complexes.

EXPERIMENTAL

Materials: All the reagents were of the best grade available and used without further purification.

Physical measurements:

Elemental analyses C, H, N and Cl analyses were determined at the Analytical Unit of Cairo University, Egypt. A standard method [gravimetric] was used to determine metal (II)/(III) ions[10]. All complexes were dried under vacuum over P_4O_{10}. The IR spectra were measured as KBr and CeBr pellets using a Perkin-Elmer 683 spectrophotometer (4000-200 cm^{-1}). Electronic spectra were recorded on a Perkin-Elmer 550 spectrophotometer. The conductances of (10^{-3} M DMF) of the complexes were measured at 25°C with a Bibby conductimeter type MCl. ^{1}H-NMR spectrum of the ligand (1) and Zn(II) complex (7) were obtained with Perkin-Elmer R32-90-MHz spectrophotometer using TMS as internal standard. Mass spectra (ligand (1) and Cu(II) complex (4)) were recorded using JEULJMS-AX-500 mass spectrometer provided with data system. The thermal analyses (DTA and TGA) of complexes Ni(II)(6), Mn(II) (9) and Bi(III) (17) were carried out in air on a Shimadzu DT-30 thermal analyzer from 27 to 700°C at a heating rate of 10°C per minute. Magnetic susceptibilities were measured at 25°C by the Gouy method using mercuric tetra thiocyanato cobalt (II) as the magnetic susceptibility standard. Diamagnetic corrections were estimated from Pascal's constant[11]. The magnetic moments

were calculated from the equation: $\mu_{eff} = 2.84\sqrt{\chi_M^{corr}.T}$. The ESR spectra of solid complexes at room temperature were recorded using a varian E-109 spectrophotometer, DPPH was used as a standard material. The T.L.C of the ligand and its complexes confirmed their purity.

Preparation of the ligand [H_3L] and its metal complexes:

Preparation of the ligand, [H_3L] (1): Ligand (1) was prepared by refluxing with stiring equimolar amounts of 4, 6 diacetyl resorcinol (10g, 0.051 mol) and anthranilic acid (7.06 g, 0.051 mol) in ethanol (50 cm^3) for 2 hours. The reddish brown product obtained was filtered off, washed several times with ethanol and dried in vacuum over P_4O_{10}. Analytical data are given in Table 1.

Synthesis of metal complexes (2)-(17): A filtered ethanolic (50 cm^3) of $Cu(OAc)_2.H_2O$ (1.99 g, 0.01 mol) was added to an ethanolic (50 cm^3) of the ligand, (1) [1L:1M] complex (2), (1.59 g, 0.01 mol) of $CuSO_4.5H_2O$ complex (3) [1L:1M], (0.99 g, 0.01 mol) of $CuCl_2.2H_2O$ complex (4) [1L:1M], (2.49 g, 0.01mol) of $Ni(OAc)_2.4H_2O$ complex (5) [1L:1M], (2.63 g, 0.023 mol) of $NiSO_4.6H_2O$ complex (6) [1L:1M], (2.19 g, 0.01 mol) of $Zn(OAc)_2.2H_2O$ complex (7) [1L:1M] (1.79 g, 0.01 mol) of $ZnSO_4.H_2O$ complex (8) [1L:1M],(2.45 g, 0.01 mol) of $Mn(OAc)_2.4H_2O$ complex (9) [1L:1M],(2.49 g, 0.01 mol) of $Co(OAc)_2.4H_2O$ complex (10) [1L:1M], (1.11 g, 0.01 mol) of $CaCl_2$ complex (11) [1L:1M], (1.83 g, 0.01 mol) 0f $CdCl_2.H_2O$ complex (12) [1L:1M], (2.78 g, 0.023 mol) of $FeSO_4$ complex (13) [1L:1M], (2.71 g, 0.01 mol) of $HgCl_2$ complex (14) [1L:1M], (4.43 g, 0.01 mol) of $Pb(OAc)_2$ complex (15) [1L:1M], (3.92 g, 0.011 mol) of $Cr_2(SO_4)_3$ complex (16) [1L:1M], (4.85 g, 0.01 mol) of $Bi(NO_3)_3.5H_2O$ complex (17) [1L:1M]. The mixture was refluxed with stirring for 1-3 hours range, depending on the nature of metal salts and the colored complex formed was filtered off, washed with ethanol and dried under vacuum over P_4O_{10}.

Antitumor evaluation:

The antitumor activity was measured *invitro* for the synthesized complexes according to Sulfo-Rhodamine-B-stain (SRB) assay using the puplished methods [12]. Cells were plated in 96-multiwell plate (10^4 cells/well) for 24 hours before treatment with the complexes to allow attachment of cell to the wall of the plate.Different concentrations of the complexes in DMSO (3.9, 7.8, 15.6, 31.25, 62.5, 125, 250 and 500 μg) were added to the cell monolayer triplicate. Monolayer cells were incubated with the complexes for 48 h at 37°C under atmosphere of 5% CO_2. After 48 h, cells were fixed, washed and stained with Sulfo-Rhodamine-B-stain. Excess stain was wash with acetic acid and attached stain was recoveredwith Tris EDTA buffer (10 m M Tris HCl + 1 m M Disodium EDTA, PH 7.5-8). Color intensity was measured by ELISA reader. The relation between surviving fraction and drug concentration is plotted to get the survival curve of each tumor cell line after the specified complex.

RESULTS AND DISCUSSION

All the complexes are stable at room temperature, non-hydroscopic, insoluble in water and partially soluble in common organic solvents such as $CHCl_3$, but soluble in DMF and DMSO. The analytical and physical data of the ligand and its complexes are given in Table 1, spectral data (Tables 2-7) are compatible with the proposed structures, (Figure 1). The molar conductances are in the 12.1-6.9 ohm^{-1} cm^2mol^{-1}range, Table 1, indicating a non-electrolytic nature[13]. The high value for some complexes suggests partial dissociation in DMF. Many attempts were made to grow a single crystal but unfortunately, they were failed. Reaction of (1) with metal salts using (1L: 1M) molar ratios in ethanol gives complexes (2)-(17). The composition of the complexes formed depends on metal salts, and the molar ratio.

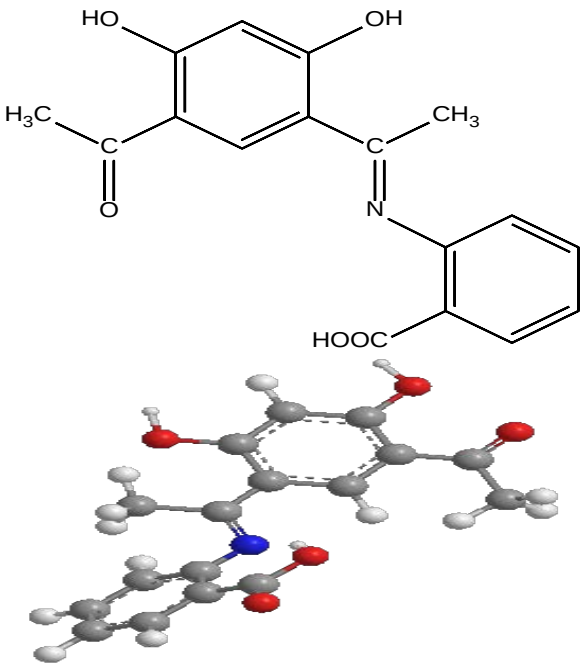

Ligand (1)

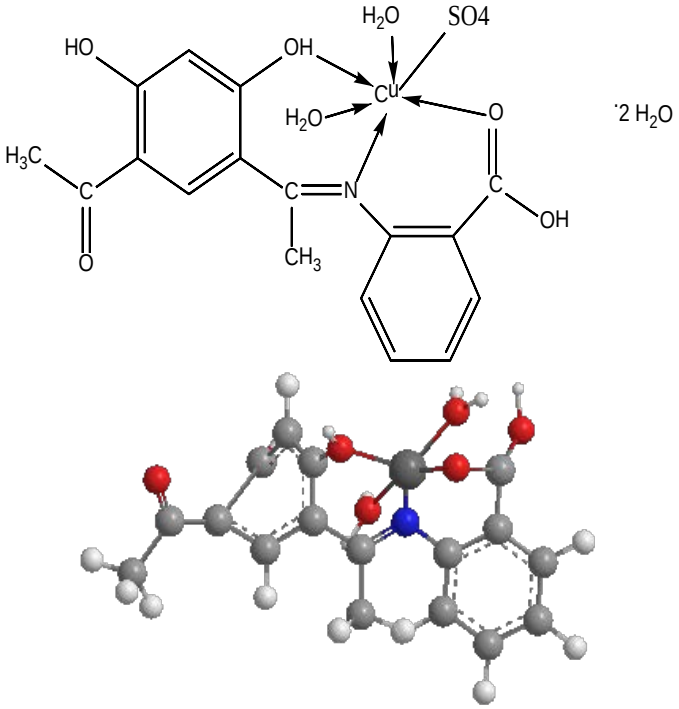

Complex (3)

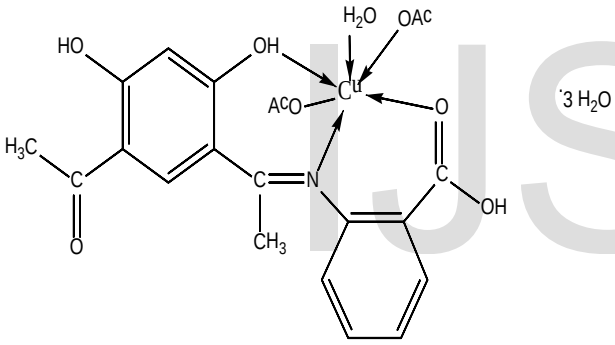

Complex (2)

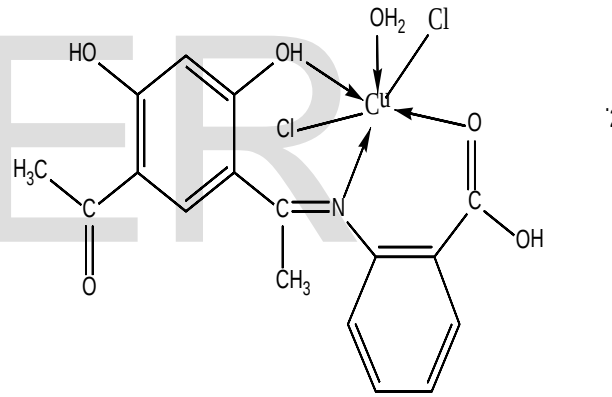

Complex (4)

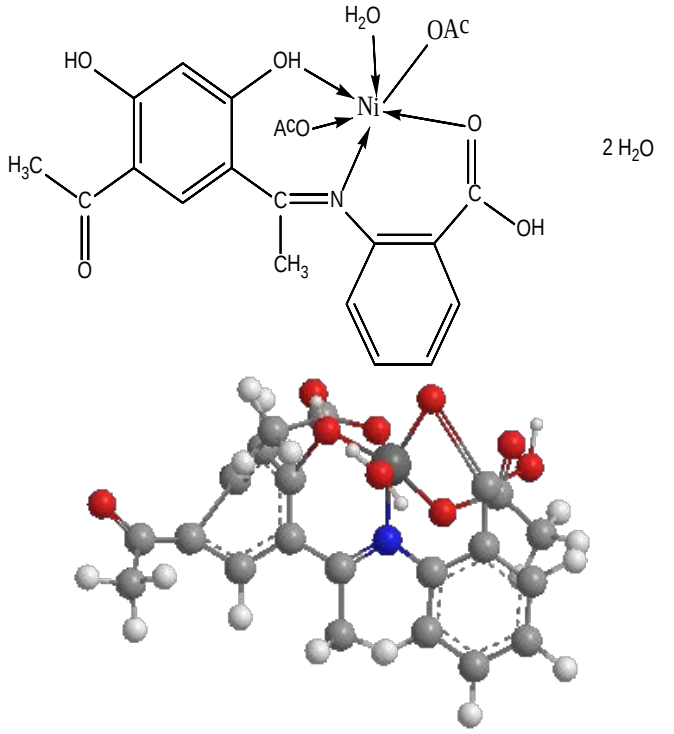

Complex (5)

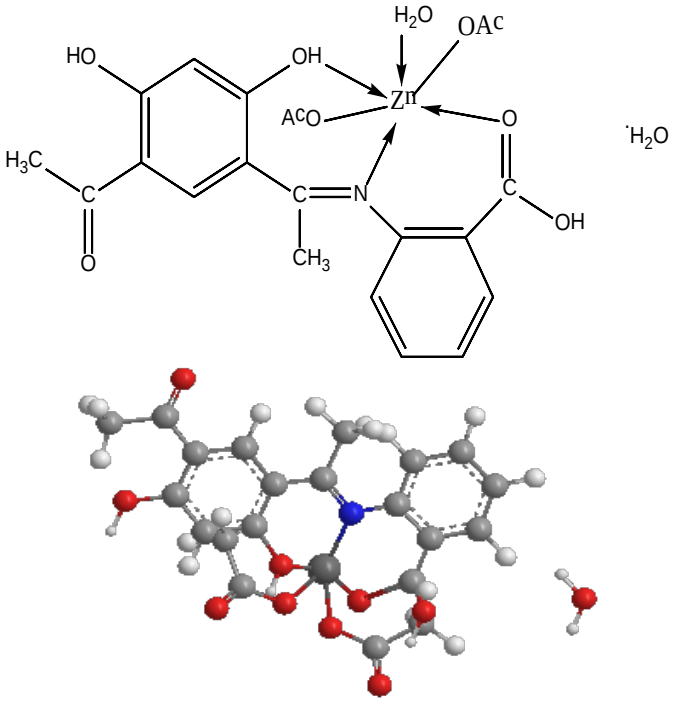

Complex (7)

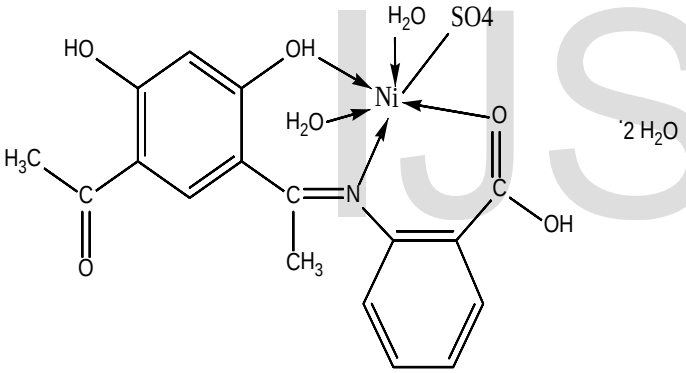

Complex (6)

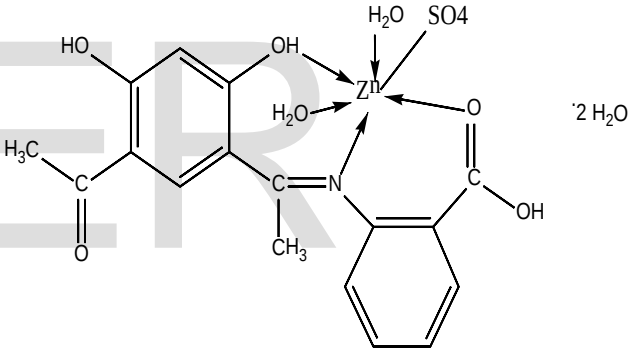

Complex (8)

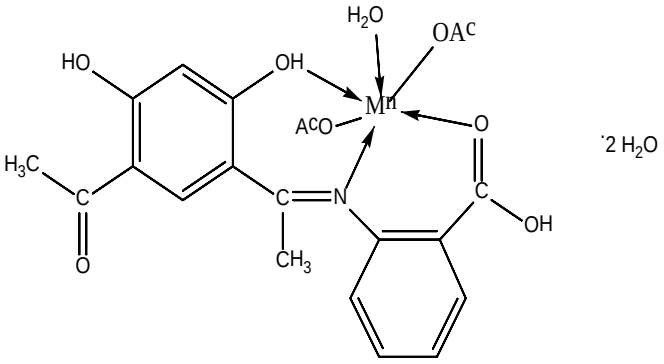

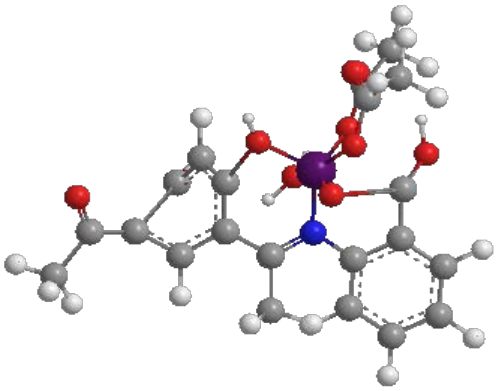

Complex (9)

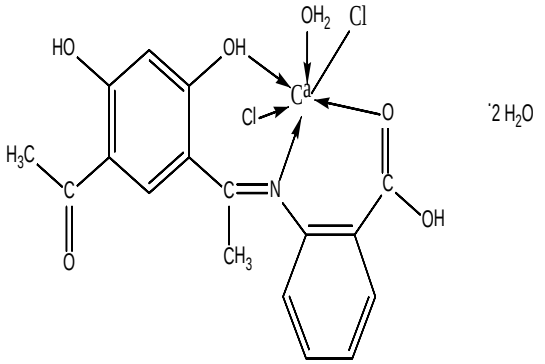

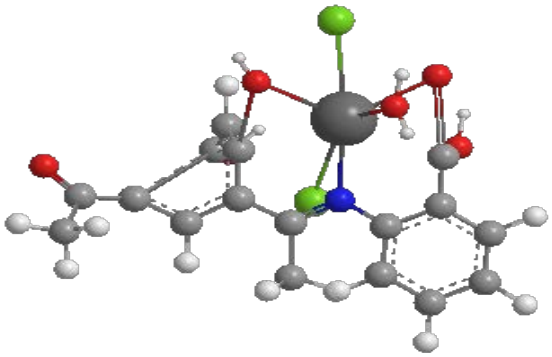

Complex (11)

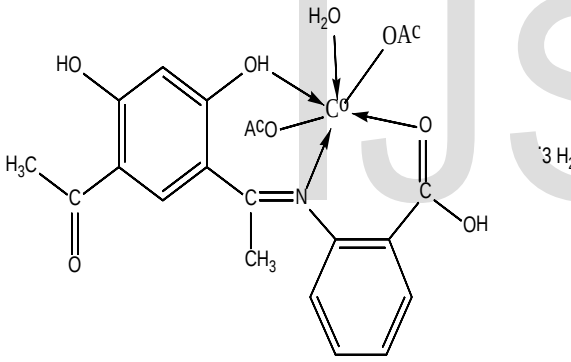

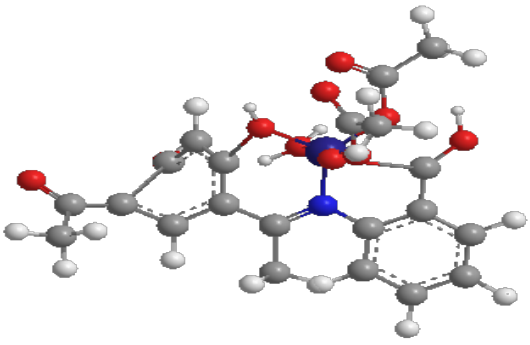

Complex (10)

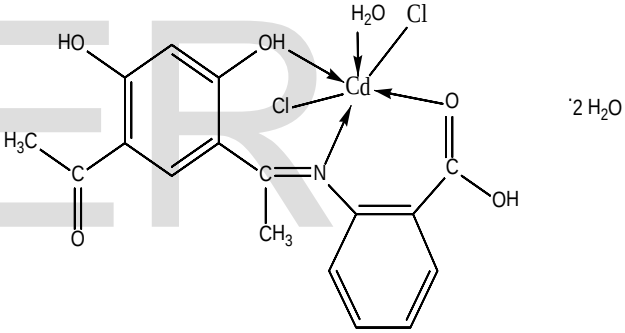

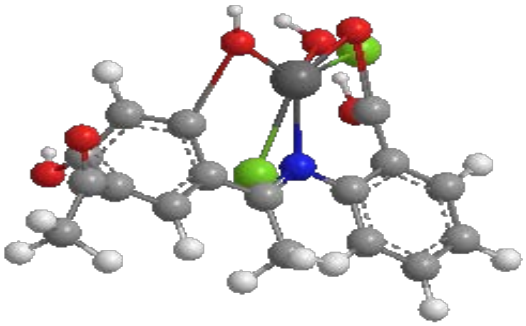

Complex (12)

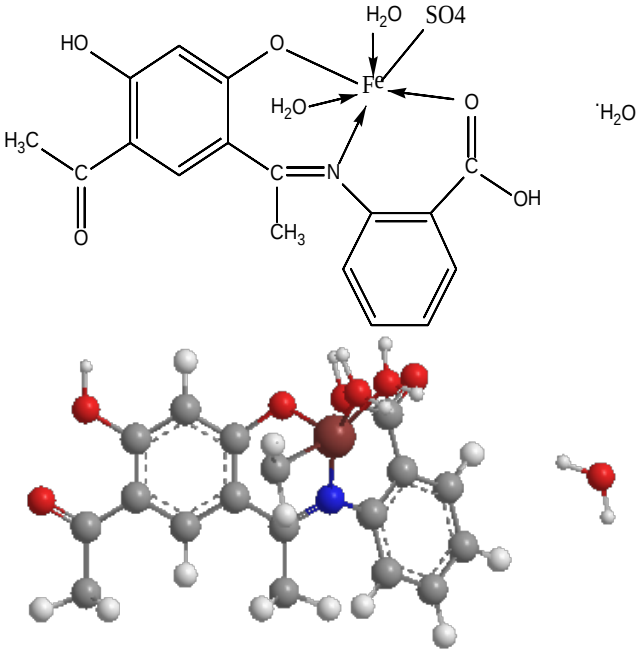

Complex (13)

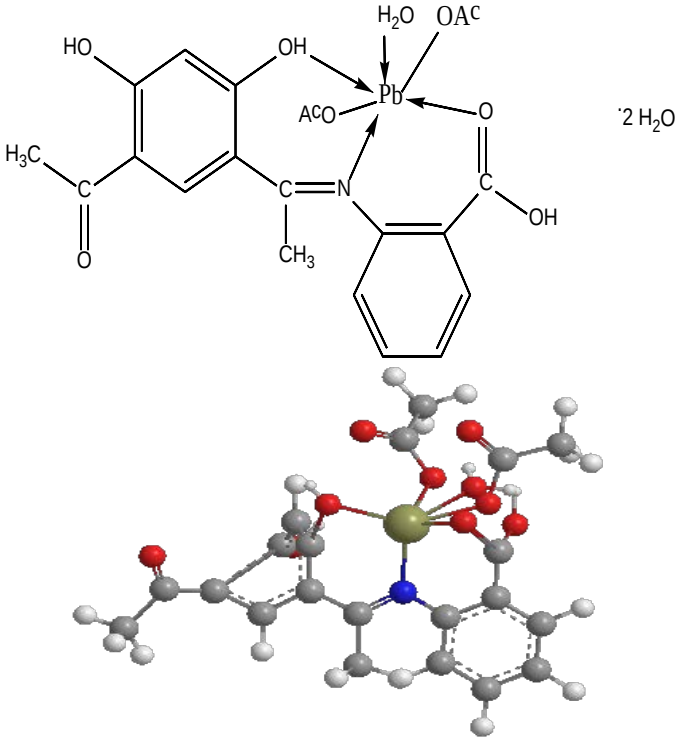

Complex (15)

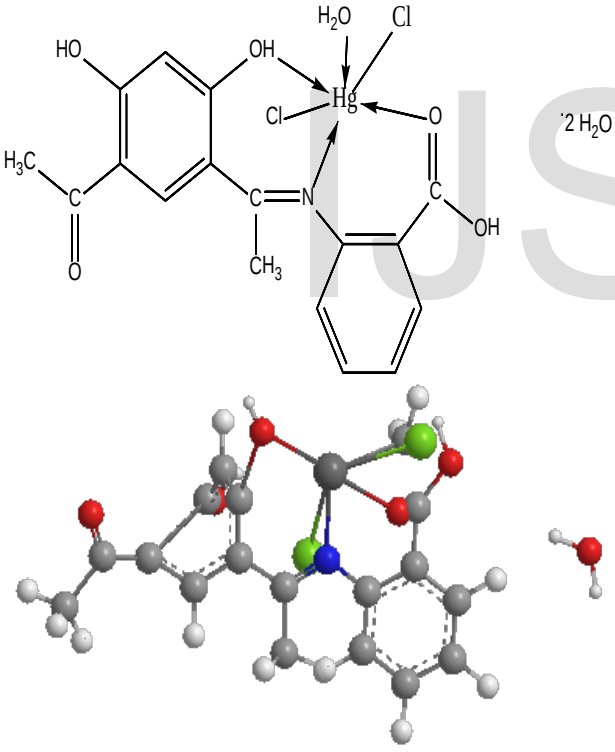

Complex (14)

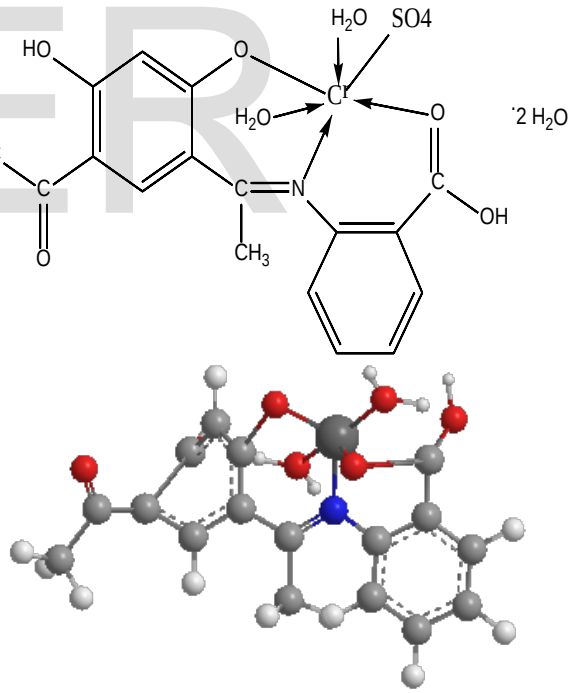

Complex (16)

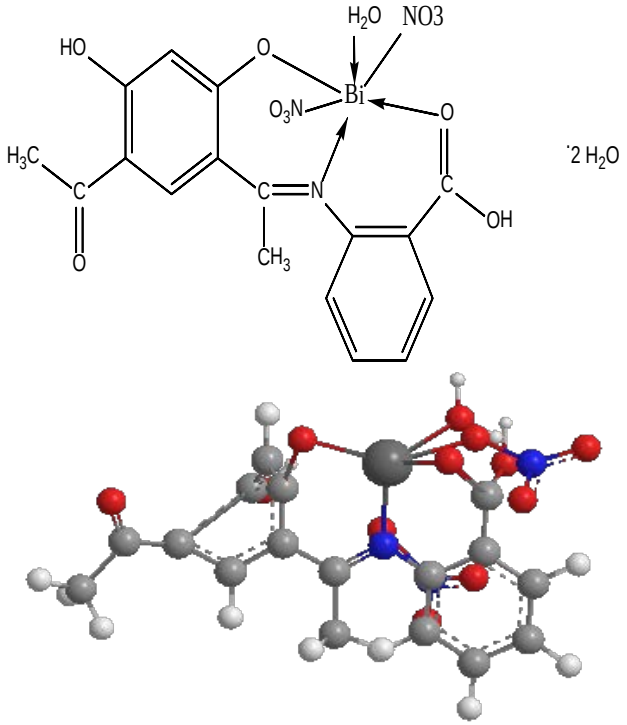

Complex (17)

Figure 1: Proposed structures of the ligand and its metal complexes

^{1}H-NMR spectra:

The ^{1}H-NMR spectrum of the ligand (1) in deuterated DMSO show signals consistent with the proposed structure. The spectrum showed a set of peaks as multiples at 6.3-8.37 ppm range which are assigned to the protons of aromatic ring[14].The chemical shift observed as a singlet at 12.7 ppm, is assigned to proton of aromatic hydroxyl group[15-17]. Methyl protons of CH_3 group appeared at 3.34 ppm as a singlet peak which was observed as multiple ones[18].

However, Zn(II) complex (7) in deuterated DMSO show signals consistent with the proposed structure. The spectrum showed a set of peaks as multiples at 6.081-8.34 ppm range which are assigned to the protons of aromatic ring. The chemical shift observed as a singlet at 12.56 ppm, is assigned to proton of aromatic hydroxyl group. Methyl protons of CH_3 group appeared at 3.3 ppm as a singlet peak. Protons of acetate group appeared at 1.86-2.084 ppm.

IR spectra:

The IR spectra of the ligand and its complexes (2)-(17) are given in Table 2. The spectrum of (1) showed ν(OH) bands at 3430 and 3380 cm^{-1}, the appearance of two broad bands at 3620-3210 and 3200-2600 cm^{-1} ranges, commensurate the presence of two types of intra-and intermolecular hydrogen-bondings[19,20]. Thus, the higher frequency band is associated with weaker hydrogen bonding and the lower frequency band with a strong hydrogen bond. Also, the spectrum shows bands at 1680, 1631 and 1253 cm^{-1} assigned to ν(C=O), ν(C=N)$_{imine}$ and ν(C-OH) respectively[21, 22, 23,24]. P-substituted aromatic ring appears at 1596, 844 and 1534, 750 cm^{-1}respectively .The IR spectra of the complexes showed, the ν(C=N)$_{imine}$ stretching frequency undergoes a shift to lower frequency by (5-20) cm^{-1}. This is indicative of nitrogen coordination of the azomethine to the metal ion[25, 26]. The ν(C=O) of carboxylic group appears in the 1650-1670 cm^{-1}, range. This vibration is located in the region of coordinated carbonyl group [25. 27]. The bands observed in the 1534-1596 and 765-870 cm^{-1} ranges are due to aromatic groups [19, 24, 25]. However, complexes (2)-(17) show medium band in the 3370-3438 cm^{-1} range is due to ν(OH) group[19, 24]. Complexes show broad bands in the 3655-3150 and 3320-2360 cm^{-1}, ranges, corresponding to intra-and intermolecular hydrogen bondings[19, 20]. However, the hydrated and coordinated water molecules appear in the 3580-3150 and 3330-2680 cm^{-1} ranges[28, 29, 30]. Extensive IR spectral studies reported on metal acetate complexes[24, 31] indicate that, the acetate ligand coordinates in either a monodentate or bidentate manner, the $\nu_a(CO_2)$ and $\nu_s(CO_2)$ of the free acetate are observed at 1560 and 1416 cm^{-1} respectively. In monodentate, the coordination of ν(C=O) is observed at higher energy than $\nu_s(CO_2)$ and ν(C-O) is appeared at lower than $\nu_{as}(CO_2)$. As a result, the separation between the two (CO) bands is much larger in unidentate than in the free ion. In complexes (2), (5), (7), (9), (10) and (15), the band is due to $\nu_{as}(CO_2)$ appears in the 1470-1425 cm^{-1} and the $\nu_s(CO_2)$ observed in the 1350-1320 cm^{-1} ranges. The difference between these two bands is in the 120-103 cm^{-1} range, suggesting that, the acetate group coordinates in unidentate manner with the metal ion[24, 31,32]. Complexes (3), (6), (8), (13) and (16) show bands at 1290, 1167, 1035 and 675, 1260, 1135, 1070 and 650, 1290, 1167 and 675, 1290, 1167, 1055 and 675, 1280, 1165, 1050 and 670 cm^{-1} respectively are corresponding to monodentate coordinate sulphate group[33]. Complexes (4), (11), (12), (14) show bands at 422, 427, 430 and 425 cm^{-1} respictively, assigened to ν(Cu-Cl)[34]. Complex (17) shows bands at 1443, 1341, 870 and 720 cm^{-1}, assigned to coordinated nitrate group [35, 36]as shown in Table 2.

Mass spectra:

The mass spectra of the ligand (1) and its Cu(II) complex (4) confirmed their proposed formulations. The spectrum of ligand reveals the molecular ion peaks (m/z) at 313 amu consistent with the molecular weight of the ligand (313.1). Furthermore, the fragments observed at m/z = 92, 119, 137, 179, 194, 256 and 313.1 correspond to C_6H_4O, C_7H_5NO, $C_7H_7NO_2$, $C_9H_9NO_3$, $C_{10}H_{12}NO_3$, $C_{15}H_{14}NO_3$ and $C_{17}H_{15}NO_5$ moieties respectively. However, the Cu (II) complex (4) shows peak (m/z) at 467.58 amu. Additionally, the peaks observed at 65, 92, 121, 152, 189, 218, 368 and 467.58 are due to C_5H_5, C_6H_6N, C_7H_7NO, $C_8H_{10}NO_2$, $C_8H_{12}ClNO_2$,

$C_9H_{13}ClNO_3$, $C_{12}H_{13}Cl_2NO_4Cu$ and $C_{17}H_{17}Cl_2NO_6Cu$ moieties respectively, as shown in Table 3.

Magnetic moments:

The magnetic moments of the complexes (2)-(17) are shown in Table 4. Cu(II) complexes (2)-(4) show values 1.69-1.71 B.M range, corresponding to one unpaired electron in an octahedral structure[31, 34]. Complex (3) shows value 1.69 B.M which is well below the spin only value (1.73 B.M), indicating that, spin-exchange interactions take place between the Cu(II) ions through intermolecular hydrogen bonding in an octahedral geometry[37]. Ni(II) complexes (5) and (6) show values 3.38 and 2.78 B.M. respectively, indicating an octahedral geometry around Ni(II) ion[38]. Mn(II) complex (9) show 5.11 B.M., suggesting high spin octahedral geometry around the Mn(II) ion[38, 39]. Co(II) complex (10) shows 4.75 B.M., indicating high spin octahedral Co(II) complexes[28, 39]. Fe(III) complex (13) shows value 5.87 B.M, suggesting high spin octahedral geometry around Fe(III) ion. Cr(III) complex (16) shows value 4.75 B.M., indicating high spin octahedral structure[39]. Zn(II), complexes (7) and (8), Ca(II) complex (11), Cd(II) complex (12), Hg(II) complex (14), Pb(II) complex (15) and Bi(III) complex (17) show diamagnetic property[19].

Table 1: Analytical and physical data of the ligand (1), [H_3L] and its metal complexes.

No.	Ligand/Complexes	Color	FW	M.P (°C)	Yield (%)	Found (Calcd.) (%) C	H	N	M	Molar conductance Λ
(1)	[H_3L] $C_7H_5NO_3$	Reddish brown	313.1	189	73	65.16 (65.0)	4.83(4.72)	4.47(4.22)	-	6.9
(2)	[$(H_2L)Cu(OAc)_2(H_2O)_2$]. $2H_2O$ $C_{20}H_{32}CuNO_{10}$	Brown	517.46	>300	65	45.66 (45.48)	4.59(4.35)	2.70 (2.5)	12.26 (12.12)	8.13
(3)	[$(H_2L)Cu(SO_4)(H_2O)_2$].$2H_2O$ $C_7H_{10}CuNO_9S$	Pale brown	511.60	>300	90	39.84 (39.61)	3.82(3.53)	2.73(2.45)	12.40 (12.25)	11.23
(4)	[$(H_2L)Cu(Cl)_2(H_2O)$].$2H_2O$ $C_{14}H_{22}CuN_2O_8$	Brown	467.58	>300	71	43.50 (43.16)	3.74(3.52)	2.98(2.7)	13.54 (13.32)	7.79
(5)	[$(H_2L)Ni(OAc)_2(H_2O)$].$2H_2O$ $C_{22}H_{37}NNiO_{12}$	Reddish brown	543.09	>300	60	46.35(46.20)	5.00(4.95)	2.57(2.37)	10.79 (10.61)	8.82
(6)	[(H_2L) $Ni(SO_4)(H_2O)_2$].$2H_2O$ $C_7H_{16}NNiO_{13}S$	Reddish brown	506.61	>300	89	40.22 (40.05)	3.85(3.68)	2.76 (2.54)	11.56 (11.32)	8.72
(7)	[(H_2L) $Zn(OAc)_2(H_2O)$].H_2O $C_{20}H_{27}NO_{12}Zn$	Brown	545.09	>300	62	48.32(48.11)	4.98(4.72)	2.56(2.37)	11.69 (11.48)	8.0
(8)	[(H_2L) Zn $(SO_4)(H_2O)_2$].$2H_2O$ $C_7H_{16}NO_{13}SZn$	Brown	512.60	>300	71	39.69 (39.51)	3.80(3.52)	2.72 (2.45)	12.71 (12.44)	8.45
(9)	[(H_2L) Mn $(OAc)_2(H_2O)$].$2H_2O$ $C_{20}H_{32}MnNO_{10}$	Dark brown	507.67	>300	92	49.66 (49.29)	4.64(4.35)	2.76 (2.41)	10.82 (10.55)	11.23
(10)	[(H_2L) $Co(OAc)_2(H_2O)$].$3H_2O$ $C_{20}H_{33}CoNO_{10}$	Pale brown	513.47	>300	63	49.10 (48.85)	4.63(4.23)	2.73 (2.38)	11.47 (11.2)	9.10
(11)	[(H_2L) $Ca(Cl)_2(H_2O)$].$2H_2O$ $C_7H_{15}CaCl_2NO_6$	Reddish brown	444.61	>300	89	45.79 (45.68)	3.93(3.72)	3.14 (3.0)	8.99 (8.89)	10.11
(12)	[$(H_2L)Cd(Cl)_2(H_2O)$].$2H_2O$ $C_7H_{15}Cd$ Cl_2NO_6	Dark brown	518.55	>300	94	39.40 (39.14)	3.38(3.09)	2.70(2.52)	21.69 (21.38)	8.89
(13)	[H_2L $Fe(SO_4)(H_2O)_2$].H_2O C_7 H_{16} Fe N O_{13} S	Dark brown	518.01	>300	73	39.40 (39.19)	3.89(3.74)	2.70(2.44)	10.78 (10.58)	11.33
(14)	[$(H_2L)Hg(Cl)_2$ (H_2O)].$2H_2O$ C_7H_{17} Cl_2 $HgNO_6$	Dark brown	606.62	>300	57	33.67 (33.50)	2.89(2.65)	2.31(2.10)	33.08 (32.87)	12.1
(15)	[$(H_2L)Pb$ $(OAc)_2$ (H_2O)].$2H_2O$ C_{11} H_{23} NO_{10} Pb	Brown	660.71	>300	92	38.20 (38.04)	3.67(3.24)	2.12(2.00)	31.38 (31.17)	10.33
(16)	[$(H_2L)Cr(SO_4)(H_2O)_2$].$2H_2O$ $C_7H_{16}CrNO_{13}S$	Light brown	499.60	>300	62	40.84(40.57)	3.71(3.50)	2.80(2.71)	10.40(10.22)	9.33
(17)	[$(H_2L)Bi$ $(NO_3)_2$ (H_2O)].$2H_2O$ C_{17} $H_{17}BiN_4$ O_{12}	Brown	667.66	>300	72	30.57 (30.41)	2.63(2.41)	6.29(6.07)	31.29(31.11)	9.87

Table 2: IR frequencies of the bands (cm^{-1}) of ligand [H_3L] and its metal complexes and their assignments.

No.	ν(Ph-O)	ν(OH)	ν(H-bonding)	ν(C=O)	ν(C=N)	ν(C-OH)	ν(Ar)	ν(OAc)/SO4/ NO3	ν(M-O)	ν(M-N)	ν(M-Cl)
(1)	-	3430, 3300	3020-3210 3200-2600	1680	1631	1283	1596, 844 1534, 750	-	-	-	-
(2)	3300-3000	3420, 3370	3635-3325, 2315-2950	1650	1625	1260	1568, 870 1540, 720	1470, 1350	543	470	-
(3)	3430-3350 3340-3000	3430, 3413	3655-3275, 3265-2760	1662	1612	1250	1563, 870 1530, 750	1290, 1167, 1035, 675	565	520	-
(4)	3520-3310 3300-2980	3438, 3411	3650-3150, 3100-2650	1667	1610	1252	1560, 866 1542, 780	-	565	525	422
(5)	3560-3315 3300-3000	3410, 3385	3630-3190, 3180-2680	1670	1618	1255	1545, 830 1525, 720	1443, 1341	540	491	-
(6)	3560-3350 3330,3000	3415, 3510	3650-3280, 3270-2450	1670	1618	1220	1560, 830 1530, 745	1268, 1135, 1070, 650	520	467	-
(7)	3650-3350 3340-3000	3430, 3415	3650-3350, 3340-2920	1659	1614	1255	1575, 785 1540, 750	1425, 1320	562	490	-
(8)	3600-3320 3330-3050	3435, 3415	3645-3450, 3140-2650	1660	1616	1252	1560, 835 1530, 760	1443, 1341	533	471	-
(9)	3520-3280 3270-3000	3430, 3411	3600-3320, 3319-2930	1665	1618	1251	1555, 830 1525, 725	1290, 1167, 1060, 675	578	535	-
(10)	3660-3315 3300-3000	3420, 3402	3650-3325, 3320-2850	1665	1630	1255	1584, 885 1535, 720	1438, 1335	537	528	-
(11)	3650-3370 3260-3000	3420, 3405	3650-3320, 3310-2650	1660	1618	1255	1592, 842 1542, 740	-	578	540	427
(12)	3635-3250 3240-2950	3418, 3407	3650-3320, 3310-2870	1665	1618	1258	1586, 865 1530, 725	-	573	475	430
(13)	3340-3280 3270-3000	3430, 3400	3648-3250, 3240-2780	1665	1620	1255	1570, 842 1545, 750	1290, 1167, 1035, 675	576	538	-
(14)	3530-3340 3330-2680	3425, 3415	3650-3330, 3310-2680	1665	1618	1254	1589, 907 1550, 780	-	578	540	425
(15)	3520-3380 3300-3090	3432	3620-3210, 3200-2780	1660	1617	1253	1537, 874 1520, 725	1439, 1330	578	540	-
(16)	3537-3338 3330-3180	3431	3650-3230, 3220-2360	1670	1610	1246	1585, 879 1550, 760	1280, 1160, 1050, 670	570	534	-
(17)	3540-3250 3240-3120	3430	3620-3320, 3310-2950	1668	1620	1250	1565, 870 1540, 760	1443, 1341, 870, 720	560	490	-

Table 3: Mass spectra of the ligand (1) and its complex (4)

Ligand/ Complex	m/z	Rel. Int.	Fragment
(1)	92	100	C_6H_4O
	119	55	C_7H_5NO
	137	39	$C_7H_7NO_2$
	179	27	$C_9H_9NO_3$
	194	8	$C_{10}H_{12}NO_3$
	256	12	$C_{15}H_{14}NO_3$
	313	6	$C_{17}H_{15}NO_5$
(4)	65	71	C_5H_5
	92	50	C_6H_6N
	121	100	C_7H_7NO
	152	40	$C_8H_{10}NO_2$
	189	28	$C_8H_{12}ClNO_2$
	218	17	$C_9H_{13}ClNO_3$
	368	13	$C_{12}H_{13}Cl_2NO_4Cu$
	467	7	$C_{17}H_{17}Cl_2NO_6Cu$

Electronic spectra:

The electronic spectral data for the ligand and its complexes in DMF solution are summarized in Table 4. Ligand in DMF solution shows two bands at 295 and 320 nm, which may be assigned to the n→π* and π→π* transitions respectively[40]. Cu(II) complexes (2)-(4) show bands in the 240– 260, 290 and 358–365 nm ranges, these bands are due to intraligand transitions, however, the bands appear in the 405–410, 531–535 and 605 –610 nm ranges are assigned to O→ Cu charge transfer, $^2B_1 \rightarrow {}^2E$ and $^2B_1 \rightarrow {}^2B_2$ transitions, indicating a distorted tetragonal octahedral structure[41-43]. Ni(II) complexes (5) and (6) show bands 256, 290, 357, 430, 560 and 732and 259,290, 360 ,435,560 and 733 nm respectively, the first three bands are within the ligand and the other three bands are attributable to $^3A_{2g}(F) \rightarrow {}^3T_{1g}(P)(\nu_3)$, $^3A_{2g}(F) \rightarrow {}^3T_{1g}(F)(\nu_2)$ and $^3A_{2g}(F) \rightarrow {}^3T_{2g}(F)(\nu_1)$ transitions respectively, indicating an octahedral Ni(II) complexes[41, 44]. The ν_2/ν_1 ratio for the complexes is 1.2 and 1.16, which are less than the usual range of 1.5–1.75, indicating a distorted octahedral Ni(II) complex[41, 45]. Mn(II) complex (9) shows bands at 251, 290, 325, 460, 570 and 620, the first three bands are within the ligand, however, the other bands are corresponding to $^6A_{1g} \rightarrow {}^4E_g$, $^6A_{1g} \rightarrow {}^4T_{2g}$ and $^6A_{1g} \rightarrow {}^4T_{1g}$ transitions which are compatible to an octahedral geometry around the Mn(II) ion[46]. Co(II) complex (10) shows bands at 267, 290, 325, 450, 565 and 617 nm, the first three bands are within the ligand and the other bands are assigned to $^4T_{1g}(F) \rightarrow {}^4A_{2g}$ and $^4T_{1g}(F) \rightarrow {}^4T_{2g}(F)$ transitions respectively, corresponding to high spin Co(II) octahedral complexes[47]. Fe (III) complex (13) shows bands at 250, 290, 312, 436, 562 and 610 nm, the first two bands are within the ligand, however, the other bands are due to charge transfer and $^6A_1 \rightarrow {}^4T_1$ transitions, suggesting distorted octahedral geometry around the iron(III) ion. While Cr(III) complex (16) shows bands at 275, 290, 311, 460, 572 and 620 nm respectively. The first three bands are within the ligand and the other bands are assigned to $^4A_{2g} \rightarrow {}^4T_{1g}$ (F), $^4A_{2g} \rightarrow {}^4T_{2g}$ and $^4A_{2g} \rightarrow {}^2T_{2g}$ transitions respectively, indicating octahedral structure around the Cr (III) ion[48, 49]. Zn(II) complex (7), (8), Ca(II) complex (11), Cd(II) complex (12), Hg(II) complex (14), Pb(II) complex (15) and Bi(III) complex (17) show three bands in the 250–290 and 310–340 nm ranges, which are assigned to intraligand transitions.

Electron spin resonance (ESR):

To obtain further information about the stereochemistry and the nature the metal ligand bonding, The ESR spectral data for complexes (2-4), (9) and (10) are presented in Table 5. ESR spectra of solid copper(II) chelates (2), (3) and (4) , are characteristic of species d^9 configuration[50,51] . The spectra showed that, the complexes exhibited anisotropic signals with g values $g_\parallel$ = 2.18, 2.19 and 2.21, $g_\perp$= 2.08, 2.072 and 2.21 respectively. These values are characteristic for a species d^9 configuration with an axial symmetry type of $d(x^2-y^2)$ ground state. The values of $g_\parallel$ and $g_\perp$ are closer to 2.00 and $g_\parallel > g_\perp > g_e$ (2.0023) indicating that, the complexes possessed a tetragonal distortion copper(II) geometry corresponding to an elongation along the four fold symmetry z-axis[52,53] . Also, the value of $g_\parallel/A_\parallel$ may be considered as a diagnostic of the stereochemistry. It has been suggested, that this quotient may be used as an empirical index of geometry. The range reported for square-planar chelates are 105-135 cm^{-1} and for tetrahedrally distorted chelates 150-250 cm. The $g_\parallel/A_\parallel$ values for the chelate under consideration lie just in the range (168-211) ranges which expected for tetragonal distorted octahedral copper (II) complexes. .In addition, the exchange coupling interaction between copper (II) ions is explained by Hathaway expression[52,54] which stated that G = $(g_\parallel - 2)/(g_\perp - 2)$. If the value of G is greater than four, the exchange interaction is negligible whereas when the value of G is less than four a considerable interaction is present in solid chelates[55]. The G values of the all copper (II) chelates are 2.5-3.0 ranges, since the interaction between copper (II) ions are present. Kivelson and Neiman noted that for an ionic environment, $g_\parallel$ is normally 2.3 or larger but for covalent environment $g_\parallel$ is less than 2.3. The values of the present chelates are less than 2.3, so there a significant degree of covalency in the metal-ligand bonding [55,56] . The σ – parameter (α^2) was calculated from the following equations

$\alpha^2 = (g_\parallel - 2.0023) + 3/7(g_\perp - 2.0023) - (P) + 0.04$ ……..(1)

Where P is the free ion dipolar term which is equal 0.036, $A_\parallel$ is the parallel coupling constant expressed in cm^{-1}. The α^2 values of the copper complexes lie in 0.57-0.71 ranges Table 5, these values indicate to the presence of a significant degree in-plane σ covalency[57,58] .

$$K_{||}^2 = (g_{||} - 2.0023)\Delta E_{xz} / 8\lambda_o$$

…… (2)

$$K_{\perp}^2 = (g_{\perp} - 2.0023)\Delta E_{xy} / 2\lambda_o$$

…… (3)

$$K^2 = (k_{||}^2 + 2k_{\perp}^2)/3$$

…….. (4)

Where λo is the spine orbit coupling of free copper ion (-828 cm^{-1}) and ΔE_{xy} and ΔE_{xz} are the electronic transition energies of $2B_1 \rightarrow 2B_2$ and $2B_1 \rightarrow 2E$ respectively[59,60]. For the purpose of calculation, it was assumed that, the maximum in the band corresponds to ΔE_{xy} and ΔE_{xz} can be taken from the wave

length of these bands. From the above relations, the orbital reduction factors ($K_{||}$, $K_{\perp}$ and K) which are a measure of covalency can be calculated[61,62]. For an ionic environment, K=1 and for a covalent environment K < 1; the lower the value of K, the greater is the covalent character. The values of K for copper complexes are less than one which inductive to considerable covalent bond character[57]. The plane and out-of-plane π-bonding coefficients (β_1^2 and β^2) respectively are dependent upon to values of ΔE_{xy} and ΔE_{xz} in the following equations:-

$$\alpha^2\beta^2 = (g_{\perp} - 2.002)\Delta E_{xy} / 2\lambda_o$$

…….…. (5)

$$\alpha^2\beta_1^2 = (g_{||} - 2.002)\Delta E_{xz} / 8\lambda_o$$

…….. (6)

The copper chelates showed β_1^2 values 0.75-0.95 range indicating a moderate degree of covalent character in the in-plane π-bonding, while β_2 are in 1.34-1.56 ranges indicating ionic character in the out-of-plane π-bonding except chelate (4), it shows > 0.83 , indicating covalent character . However, manganese (II) chelate (9) and cobalt chelate (10) show isotropic type with g iso = 2.07 and 2.05 respectively, indicating octahedral structure around their ions .It is possible to calculate approximate d orbital population using the following equation.

$$A_{||} = Aiso - 2B\,[1 \pm (7/4)\Delta g_{||}$$

$$a^2d = 2B/2B^o$$

Where $2B^o$ is the calculated dipolar coupling for unit occupancy of d orbital .When the data are analyzsed using the Cu[63] hyperfine coupling and considered all the sign combinations. The orbital populations for complexes (2),(3), and (4) are 57%,60% and 93% respectively, indicating a $d_{(x2-y2)}$ ground state .

Table 4: The electronic absorption spectral bands (nm) and magnetic moment (B.M.) for the ligand [H_3L] and its complexes

No.	λ_{max} (nm)	μ_{eff} in B.M.
(1)	295,320	-
(2)	260, 290 , 420,533, 610	1.71
(3)	260, 290, 405,533, 605	1.69
(4)	240, 290,410, 531,610	1.67
(5)	256, 290, 357,430,560,732	3.38
(6)	259,290, 360 ,435,560,733	2.78
(7)	250, 290, 340	Diam.
(8)	265,290, 310, 700	Diam.
(9)	251, 290, 325, 460, 570, 620	5.11
(10)	267, 290, 325, 450, 565, 617	4.75
(11)	270, 290, 315	Diam.
(12)	260, 290, 310	Diam.
(13)	250, 290, 312, 436, 562, 610	5.78
(14)	262, 290, 316	Diam.
(15)	267, 290, 317	Diam.
(16)	275, 290, 311, 460, 572, 620	4.75
(17)	255, 290, 310	Diam.

Table 5: ESR data for the metal (II) complexes

No.	$g_{||}$	$g_{\perp}$	g_{iso}[a]	$A_{||}$ (G)	$A_{\perp}$ (G)	A_{iso}[b] (G)	G[c]	ΔE_{xy}	ΔE_{xz}	$K_{||}^2$	$K_{\perp}^2$	K	$g_{||}/A_{||}$	α^2	β^2	β_1^2	-2 β	a_d^2 (%)
(2)	2.18	2.08	2.11	125	12.5	50	2.5	17241	20408	0.95	0.46	0.88	169.7	0.61	1.56	0.75	133.6	57
(3)	2.19	2.072	2.11	130	10	50	2.68	18691	20618	0.83	0.52	0.85	168.46	0.62	1.34	0.84	140	60
(4)	2.21	2.07	2.11	100	10	40	3.0	18832	24390	0.99	0.59	0.92	211	0.56	0.57	0.95	218.7	93
(9)	-	-	2.07	-	-	-	-	-	-	-	-	-	-	-	-	-	-	-
(10)	-	-	2.05	-	-	-	-	-	-	-	-	-	-	-	-	-	-	-

a) $g_{iso} = (2g_{\perp} + g_{||})/3$, b) $Aiso = (2A_{\perp} + A_{||})/3$, c) $G = (g_{||} - 2)/(g_{\perp} - 2)$

Thermal analyses (DTA and TGA):

The thermal curves in the temperature 27-700°C range for complexes (6), (9), and (17) are thermally stable up to 40°C. Breaking of hydrogen bondings occur as endothermic peak within the temperature 45-50°C as shown in Table 6. Complexes show decomposition step within temperature 80-98°C range, is due to elimination of hydrated water molecules[63, 64] ($2H_2O$). Another thermal decomposition appeared at 117°C, is due to loss of two coordinated water molecules (H_2O) complex (6), one coordinated water molecule at 102°C and 180°C for complex (9) and (17) respectively. Complex (6) shows one endothermic peak at 222°C with 20.39% weight loss (Calc. 20.15%), corresponding to the loss of one coordinated sulphate group. Endothermic peak observed at 330°C may be due to melting point. Finally, the complex shows exothermic peaks at 380, 445 and 530 °C with 18.19% weight loss (Calc. 18.04%), corresponding to oxidative thermal decomposition which proceeds slowly with final residue at 650°C, assigned to NiO[63]. Complex (9) shows endothermic peak at 173 °C

with 23.9% weight loss (Calc. 24.1%), is due to loss of two coordinated acetate groups. The endothermic peak observed at 273°C may be due to melting point. Oxidative thermal decomposition occurs at 315, 367, 430, 530 and 610 °C with 11.31% weight loss (Calc. 11.33%), with exothermic peaks, leaving MnO[65]. Complex (17) shows endothermic peak at 231°C with 19.04% weight loss (Calc. 19.11%), is due to loss of two nitrate group. Also, another endothermic peak observed at 280°C is due to melting point. Oxidative thermal decomposition occurs at 334, 375, 435, 520 and 630 °C with 41.21% weight loss (Calc. 41.44%), with exothermic peaks, leaving BiO. The thermal data are present in Table 6.

Table 6: Thermal data for the metal complexes

No.	Temp. (°C)	DTA(Peak)		TGA (wt. loss %)		Assignment
		Endo	Exo	Calc.	Found	
(6)	50	Endo	-	-	-	Breaking of H-bonding
	97.8	Endo	-	7.10	17.02	Loss of two hydrated water molecules
	117.1	Endo	-	7.64	7.48	Loss of two coordinated water molecules
	222	Endo	-	20.39	20.15	Loss of one sulphate group
	330	Endo	-	-	-	Melting point
	380, 445,530,650	-	Exo	18.19	18.04	Decomposition process with formation NiO
(9)	45	Endo	-	-	-	Breaking of H-bonding
	80	Endo	-	7.09	7.00	Loss of two hydrated water molecules
	102	Endo	-	3.81	3.74	Loss of one coordinated water molecules
	173	Endo	-	24.1	23.9	Loss of two coordinated acetate groups
	273	Endo	-	-	-	Melting point
	315, 367.8, 430, 530,610	-	Exo	11.33	11.31	Decomposition process with formation of MnO
(17)	50	Endo	-	-	-	Breaking of H-bonding
	96.7	Endo	-	5.40	5.37	Loss of two hydrated water molecules
	180	Endo	-	2.85	2.75	Loss of one coordinated water molecules
	230.9	Endo	-	19.11	19.04	Loss of two nitrate groups
	280	Endo	-	-	-	Melting point
	334.5, 375, 435,520, 630	-	Exo	41.44	41.21	Decomposition process with formation of BiO

Antitumor studies:

The antitumor effect of metal complexes (7), (8) and (12) in DMSO were evaluated against human breast cancer MCF-7 cell line. These were tested by comparing them with the standard drug (IMURAN (azathioprine)). The solvent DMSO showed no effect on cell growth as it reported previously[66]. The metal complexes showed moderate effect against MCF-7 cell lines. There was a positive correlation between the surviving fraction ratio of MCF-7 tumor cell line and the concentration. The Zn(II) complex (8) showed a high potency of inhibition (89.47%) at 500µg/ml against MCF-7 tumor cell line, (81.04%) at 250µg/ml compared with a standard drug. Also, the Cd(II) complex (12) showed a high potency of inhibition (71.31%) at 500µg/ml against MCF-7 tumor cell line, (52.38%) at 250µg/ml, compared with a standard drug[65]. Also, the Zn(II) complex (7) showed inhibition of (61.39%) at 500µg/ml against MCF-7 tumor cell line, (47.63%) at 250µg/ml compared with a standard drug, as shown in Figure (2), Figure (3). This could be explained as follow Zn(II) and Cd(II) could bind to DNA where it seemed that, change the anion and the nature of the metal ion in complexes may have effect on the biological behavior, by altering the binding ability of DNA[66-70]. Moreover, Gaetke and Chow had reported that, metal has been suggested to facilitate oxidated tissue injury through a free-radical mediated pathway analogous to the Fenton reaction[71]. By applying the ESR-trapping technique, evidence for metal-mediated hydroxyl radical formation invivo has been obtained. Radicals are produced through a Fenton-type reaction as follows[71]:

$$LM(II) + H_2O_2 \rightarrow LM(I) + {}^{\cdot}OOH + H^+$$

$$LM(I) + H_2O_2 \rightarrow LM(II) + {}^{\cdot}OH + OH^-$$

Where L is the ligand

Also, metal could act as a double-edged, sword by inducing DNA damage and also by inhibiting their repair[72]. The OH radicals react with DNA sugars and bases and the most significant and well-characterized of the OH reactions is hydrogen atom abstraction from the C_4 atom to yield sugar radicals with subsequent β-elimination. (Scheme 1), by this mechanism strand breakage occurs as well as the release of the free bases[73-75]. Another form of attack on the DNA bases is by solvated electrons, probably via a similar reaction to those discussed below for the direct effects of radiation on DNA[76, 77].

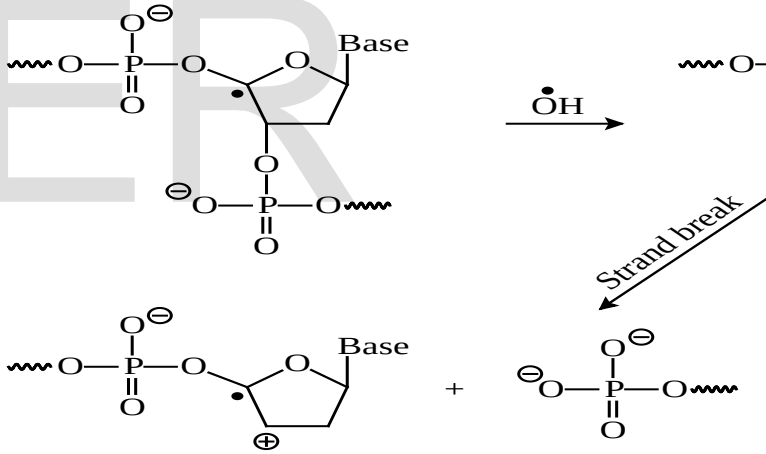

Scheme (1)

The IC_{50} values were in the (50-293) µg range against human breast cancer MCF-7 cell line. Zn(II) complex (8) demonstrated the highest potency inhibition activity among all tested compounds against MCF-7 cell line with IC_{50} (50.2)..The relation between the concentration of the complexes in DMSO and their antiproliferative.

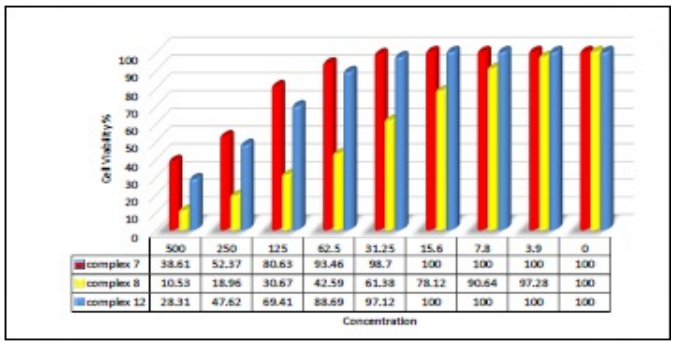

Figure (2): Evaluation of cytotoxicity of metal complexes against breast cancer MCF-7 cell line

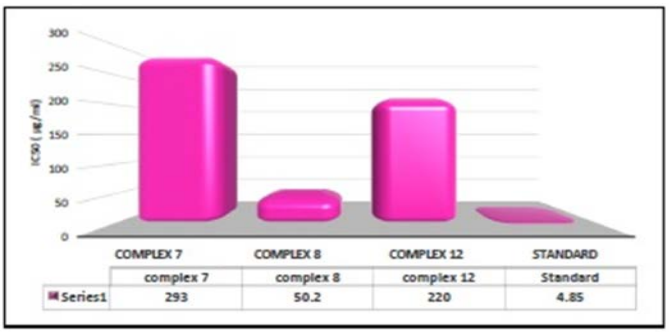

Figure (3): IC50 values of the metal complexes against breast MCF-7 cancer cell lines

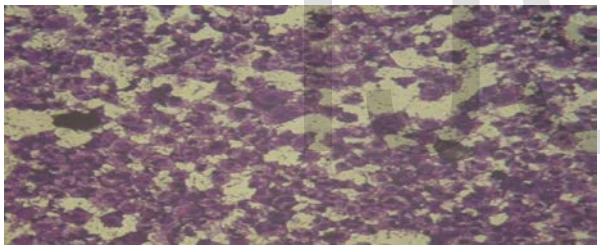

Histogram of MCF-7 cells treated with complex (8) at 62.5 µg/ml

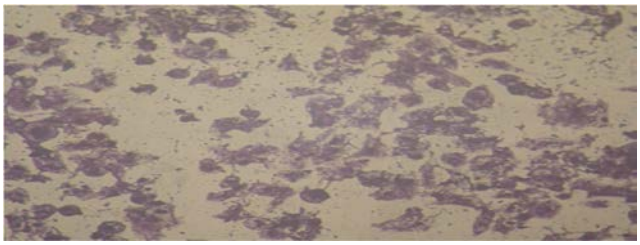

Histogram of MCF-7 cells treated with complex (8) at 125 µg/ml

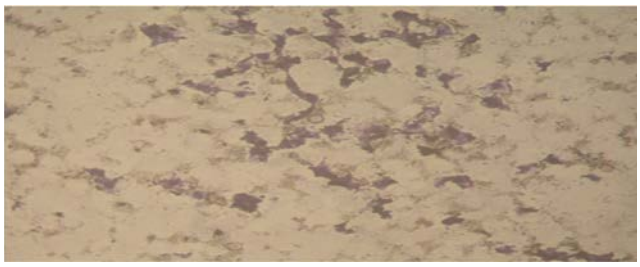

Histogram of MCF-7 cells treated with complex (8) at 250 µg/ml

Histogram of MCF-7 cells treated with complex (8) at 500 µg/ml

Figure 4: Histogram of MCF-7 cells treated with complex (8) at different concentrations

Conclusion:

Cr (III), Mn (II), Co (II), Ni (II), Cu (II), Zn (II), Cd (II), Ca(II), Fe(III), Hg(II), Pb(II), and Bi(III) complexes of (E)-2-((1-(5-acetyl-2,4-dihydroxy phenyl) ethylidene) amino) benzoic acid were prepared and characterized by elemental analyses, IR, UV-Vis spectra, Magnetic moments, Conductivity, ^{1}H-NMR and Mass spectra, Thermal analyses (DTA and TGA) and ESR measurements. The analytical and IR data showed that, the ligand behaves as neutral monobasic tridentate. Molar conductivity in DMF indicate that, the complexes are non-electrolytes. ESR spectra of solid Cu(II) complexes at room temperature show axial type (dx^2-y^2) with covalent bond character in an octahedral environment. However, Co(II), Fe(III) and Mn(II) complexes showed isotropic type. Complexes showed inhibitory activity against human breast cancer (MCF-7 cell line) compared with standard drug. Also, the Zn(II) complex (8) showed a high potency of inhibition (89.47%) at 500µg/ml against MCF-7cell line, (81.04%) at 250µg/ml, (69.33%) at 125µg/ml compared with a standard drug. Zn(II) complex (8) demonstrated the highest potency inhibition activity among all tested compounds against MCF-7 cell line with IC_{50} (50.2) µg.

Acknowledgement:

The authors express their sincere gratitude to Academy of Scientific Research and Technology (Cairo, Egypt) for their financial support for the research.

REFERENCES:

1. A. A. El-Asmy, O. A. El-Gammal and H. A. Radwan; *Spectrochim. Acta, Part A*, 76,496 (2010).
2. Magdy. A. Wassel, Abdou. S. El-Tabl, Ahmed. S. El-zaref and Mahmoud. M. Arafa; I*nt.J. of Science and Research*, vol. 6, 912 (2017).
3. Magdy. A. wassel, Abdou. S. El-Tabl, Moshira. M. Abd EL-Wahed, Anwar. A. Wassel and Mahmoud. M.

Arafa; *Int. J. of scientific and Engineering*, 9, 2151 (2018).
4. R. M. El-Bahnasawy, A.S.El-Tabl, E. El-Shereafy, T. I. Kashr and Y. M. Issa; *Polish J.Chem*, 73,1952 (1999).
5 A. S. El-Tabl, F. A. EL-Saied and A. N. Al- Hakimi; *Trans. Met Chem*, 32, 701 (2007).
6. B. Murukan and K. Mohanan, *Trans. Met. Chem*, 31, 441 (2006).
7. S. N. Pandeya, S. Smitha, M. Jyoti, and S. K. Sridhar; *Acta Pharm*, 55, 27 (2005).
8. T. I. Kashar, A. S. El- Tabl and R. M. El- Bahnasawy,; *Polish J. Chem*, 72, 2037 (1998).
9. C. Loncle, J. M. Brunel, N. Vidal, M. Dherbomez and Y. Letourneux; *Eur. J. Med. Chem*, 39, 1067 (2004).
10. S. G. Kucukguzel, A. Maz, F. Sahim, S. Öztürk and J. Stables; *Eur. J. Med. Chem*. 38, 1005 (2003).
11. R. Todeschini, A. L. P. de Miranda, K. C. M da silva, S. C. Parrini and E. J. Barrciro; *Eur.J. Med. Chem*. 33, 189 (1998).
12. P. Melnyk, V. Leroux, C. Scrgheraret, and P. Grellier; *Bioorg. Med. Chem. Lett*, 16, 31(2006).
13. P. C. Lima, L. M .LIMA, K. C. M.dasilva, P. H. O. Leda, A. L. P. de Miranda, C. A. M. Fraga and E. J. Barreiro; *Eur. J. Med. Chem*, 35, 187 (2000).
14. C. Cunha, J. M. Figuciredo, J. L. M. Tributino, A. L. P. Miranda, H. C. Castro, R. B.Zingal, C.A.M. Fraga, M. C. B. V. de souza, V. F. Ferrcira and E. J. Barreiro; *Bioorg. Med. Chem*, 11, 205 (2003).
15. A. S. EL-Tabl, F. A. Aly, M. M. E. shakdofa and A. M. E. Shakdofa; *J, Coord. Chem*, 63,700 (2010).
16. B. S. Tovrog, D. J. kitko and R. S. Dragom, *J. Am. Chem. Soc*., 98, 5144 (1976).
17. N. Batra and J. Devi, *J. Chem. Pharma. Res*., 7, 183 (2015).
18. Y. Xiao, C. Bi, Y. Fan, S. Liu, X. Zhang, D. Zhang, Y. Wang and R. Zhu, *J. Coord. Chem,* 62, 3029 (2009).
19. E. I. Solomon, M. D. Lowery, "Electronic structure contributions to function in bioinorganic chemistry" *Science,* 259 (5101), 1575–1581 (1993).
20. M. Tümer, E. Akgün, S. Toroglu, A. Kayraldız and L. Dönbak, *J. Coord. Chem*., 61(18), 2935– 2949 (2008).
21. A. Gölcü, M. Tümer, H. Demirelli and R. A. Wheatley, *Inorg. Chim. Acta,* 358, 785–1797 (2005).
22. G. Svehla, Vogel's Textbook of macro and semimicro qualitative inorganic analysis, Longman London, (1979).
23. F. J. Welcher, analytical uses of ethylene diaminetetraacetic acid, (1958).
24. A. A. Vogel, Text Book of Quantitative Inorganic Analysis, ELBS, London (1978).
25. B. Figgis, J. Lewis and R. Wilkins, Modern coordination chemistry, *Interscience*, New York, 403 (1960).
26. S. Shieh, C. Che and S. Peng, *Inorg. Chim. Acta,* 192, 151 (1992).
27. D. Mishra, S. Naskar, M. C. B. Drew and S. K. Chattopadhyay, *Inorg. Chim. Acta,* 359,585(2006).
28. A. S. El-Tabl, M. M. Abd El-Wahed and A. M. S. Rezk, Spectrochim, *Acta, Part A*, 117,772-788 (2014).
29. A. S. El-Tabl, W. Plass, A. Buchholz and M. M. Shakdofa, *J. Chem. Res*., 582 (2009).
30. M. R. Maurya, S. Khurana, C. Schulzke and D. Rehder, Eur. *J. Inorg. Chem*.779-788 (2001).
31. M. R. Maurya, S. Agarwal, C. Bader and D. Rehder, *Eur. J. Inorg. Chem.,* 147-157 (2005).
32. A. S. El-Tabl, F. A. El-Saied and A. N. Al-Hakim, *Trans. Met. Chem*.32, 689 (2007).
33. A. S. El-Tabl, M. M. E. Shakdofa, A. M. A. El-Seidy, *Korean J. Chem. Soc*.,55,603 (2011).
34. M. M. Aly, S. M. Imam, *Montash Chem*., 126, 137 (1995).
35. A.S. El-Tabl, T. L. Kashar, R.M. El-Bahnasay, A. El-Mohsef, *Polish J.Chem*., 73, 245 (1999).
36. A. S. El-Tabl, *Trans. Met. Chem*., 27, 166 (2002).
37. Nakatamato, Infrared Spectra of Inorganic and Coordination compounds, second ed.Wiley, New York, (1971).
38. H. A. Kuska, M. T. Rogers, in: A. E. Martell (Ed), Coordination Chemistry, vol. 92, Van Nos Trad Reihoid Co., New York, 1971.
39. M. F. R. Fouda, M. M. Abd-El-Zaher, M.M. Shakdofa, F.A. El-Sayed, M.I. Ayad and A.S. El-Tabl, *J. Coord. Chem*., 61, 1983 (2008).
40. H. A. Kuska and M. T. Rogers, in: *A.E. Martell (Ed), Coordination Chemistry*, vol. 92, Van Nos- trad Reihoid Co., New York, (1971).
41. A. S. El-Tabl, *Trans. Met Chem*., 27, 166 (2002).
42. A. S. El-Tabl, *J. Chem. Res*., 529-531 (2002).
43. R. M. El-Bahnasawy, A. S. El-Tabl, E. El-Sheroafy, T. I. Kashar and Y. M. Issa, *Polish J.Chem*., 73 (1995).
44. K. B. Gudasi, S. A. Patel, R. S. Vadvavi, R. V. Shenoy and M. Nethayi, *Trans. Met. Chem*., 31, 580-585 (2006).
45. A. S. El-Tabl, F. A. El- Said, A. N. Al-Hakim, *Trans. Met. Chem*.,67, 265 (2007).
46. N. A. Al-Hakimi, M. M. E. Shakdofa, A. M. A. El-Saidy and A. S. El-Tabl, *J. Korean Chem. Soc*., 55, 418 (2011).
47. A. S. El-Tabl, *Transition Met.Chem*, 22, 400-405 (1997).
48. A. E. Motaleb, M. Ramadan, W. Sawondy, H. Baradie and M. Gaber, *Trans. Met. Chem*., 22, 211, 215 (1997).
49. A. S. El-Tabl, S. A, El-Enein, *J. Coord. Chem*., 57, 281 (2004).
50. S. A. Sallam, A. S. Orabi, B. A. El-Sheraty and A. Lentz, *Trans. Met. Chem*., 27,447 (2002).
51. B. H. Krishna, C. M. Mahapatra and K. C. Dush, *J.*

Inorg. Nucl. Chem., 39, 1253 (1997).
52. A. S. El-Tabl, F. A. El-Saied and A. N. Al-Hakimi, *J. Coord. Chem.*, 61, 2380 (2008).
53. N. K. Singh and S. B. Singh, *Trans. Met. Chem.*, 26, 487 (2001).
54. R. K. Parihari and R. K. Patel, *J. Ind. Chem. Soc.*, 77, 339 (2000).
55. N. V. Takkar and S. Z. Bootwala, *Ind. J. Chem.*, 34A, 370-374 (1995).
56. G. C. Chinvmia, D. G. Phillips and A. D. Rae, *Inorg. Chim. Acta*, 238, 197-201 (1995).
57. A. S. El-Tabl, *Bull. Korean Chem. Soc.*, 25, 1-6 (2004).
58. A. S. El-Tabl, M. M. E. Shakdofa and A. M. A. El-Seidy, *Korean J. Chem. Soc.*, 55, 603 (2011).
59. H. A. El-Boraey and A. S. El-Tabl, *Polish J. Chem.*, 77, 1759-1775 (2003).
60. A. S. El-Tabl, *Trans. Met. Chem.*, 23, 63 (1998).
61. I. M. Procter, B. J. Hathaway and P. N. Nicholls, *J. Chem. Soc. A*, 1678-1684 (1969).
62. D. E. Nikles, M. J. Powers and F. L. Urbach, *Inorg. Chem.*, 22, 3210 (1983).
63. R. K. Ray, *J. Inorg. Chim. Acta*, 174, 257 (1990).
64. D. W. Smith, *J. Chem. Soc. A*, 22, 3108 (1970).
65. A. S. El-Tabl, *J. Chem. Res.*, 19 (2004).
66. D. Kivelson and R. Neiman, *J. Chem. Phys.*, 35, 149 (1961).
67. H. A. El-Boraey, A. S. El-Tabl, *polish J. Chem.*, 77, 1759 (2003).
68. M. M. Bhadbhade and D. J. Srinivas, *Inorg. Chem.*, 32, 2458 (1993).
69. A. S. El-Tabl and S. M. Imam, *Trans. Met. Chem.*, 22, 259 (1997).
70. M. Gaber and M. M. Ayad, Thermochim, *Acta*, 176, 21-29 (1991).
71. A. S. El-Tabl and M. M. Abou-Sekkina, *polish J. Chem.*, 73, 1937 (1999).
72. A. S. El-Tabl, M. M. Abou-Sekkina, *Polish J. Chem.*, 73, 937-1945 (1999).
73. V. Vichai and K. Kirtikara, *Nature Protocols*, 1112 – 1116 (2006).
74. A. S. El-Tabl, M. M. Abd El-Waheed, M. A.Wahba and N. A. Abou El-Fadl, *Bioinorg. Chem. Appl.*, 1-14 (2015).
75. A. Nicodemo, M. Araujo, A. Ruiz, A. Gales, 53(4), 604-608 (2004).
76. Standards, N. C. f. C. L. Performance standards for antimicrobial disk and dilution susceptibility tests for bacteria isolated from animals. *Approved standard*. vol M31-A2.NCCLS, Wayne, Pennsylvania, (2001).
77. J. G. Collee, J. P. Duguid, A. G. Farser and B. D. Marmion e.(eds) Practical medical microbiology. Churchill Livingstone, New York, (1989).

Corresponding author: Abdou Saad El-Tabl
Chemistry Department, Faculty of Science, Menoufia University, Shebin El-Kom, Egypt